

Falcon: Accelerating Homomorphically Encrypted Convolutions for Efficient Private Mobile Network Inference

Tianshi Xu^{1,2}, Meng Li^{1,2*}, Runsheng Wang^{1,3,4}, Ru Huang^{1,3,4}

¹ School of Integrated Circuits, Peking University, Beijing, China

² Institute for Artificial Intelligence, Peking University, Beijing, China

³ Institute of Electronic Design Automation, Peking University, wuxi, China

⁴ Beijing Advanced Innovation Center for Integrated Circuits, Beijing, China

meng.li@pku.edu.cn

Abstract—Efficient networks, e.g., MobileNetV2, EfficientNet, etc, achieves state-of-the-art (SOTA) accuracy with lightweight computation. However, existing homomorphic encryption (HE)-based two-party computation (2PC) frameworks are not optimized for these networks and suffer from a high inference overhead. We observe the inefficiency mainly comes from the packing algorithm, which ignores the computation characteristics and the communication bottleneck of homomorphically encrypted depthwise convolutions. Therefore, in this paper, we propose Falcon, an effective dense packing algorithm for HE-based 2PC frameworks. Falcon features a zero-aware greedy packing algorithm and a communication-aware operator tiling strategy to improve the packing density for depthwise convolutions. Compared to SOTA HE-based 2PC frameworks, e.g., CrypTflow2, Iron and Cheetah, Falcon achieves more than $15.6\times$, $5.1\times$ and $1.8\times$ latency reduction, respectively, at operator level. Meanwhile, at network level, Falcon allows for 1.4% and 4.2% accuracy improvement over Cheetah on CIFAR-100 and Tiny Imagenet datasets with iso-communication, respectively.

Index Terms—Secure Two-Party Computation, Homomorphic Encryption, Depthwise Convolution, Convolution Packing

I. INTRODUCTION

Recent years have witnessed the algorithmic breakthroughs as well as the compute and parameter explosion of convolutional neural networks (CNNs). State-of-the-art (SOTA) efficient networks, e.g., MobileNetV2 [1], EfficientNet [2], ConvNext [3], etc, achieve superhuman accuracy with lightweight computation. Therefore, they are getting increasingly adopted in real-world applications, including sensitive and private tasks such as face authentication [4], medical diagnosis [5], etc. Privacy has thus emerged as a major concern in the network deployment and there is a growing demand for privacy-preserving deep neural network (DNN) inference [6]–[9].

Homomorphic encryption (HE)-based secure two-party computation (2PC) helps solve the following dilemma: the server, who owns a private model, and the client, who owns private data, want to jointly apply the model to the data without giving out the model or data. HE-based 2PC not only

This work was supported in part by the NSFC (62125401) and the 111 Project (B18001).

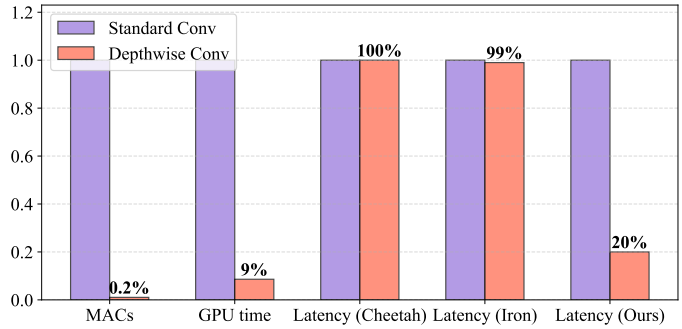


Fig. 1. Compare a depthwise convolution with a standard convolution on compute (measured by multiplication accumulations, i.e., MACs), latency on GPU, as well as latency of two prior-art and our 2PC frameworks.

enables the inference but also permits a cryptographically-strong privacy protection, attracting a lot of attention in recent years [10]–[12].

As CNNs process high-dimensional tensors while HE computes over polynomials, the first step of HE-based inference is the mapping from tensors to polynomials, whose coefficients are usually regarded as a one-dimensional vector, denoted as packing [13]. The packing algorithm directly impacts the inference correctness and complexity and has been widely studied to improve the HE-based 2PC efficiency for CNNs [10], [13]–[17].

However, existing HE-based 2PC frameworks are not optimized for efficient networks, which extensively use depthwise and group convolutions to reduce the compute and latency [1], [2], [18], [19]. As shown in Figure 1, in two prior-art 2PC frameworks, the latency of a depthwise convolution is almost the same as a standard convolution, indicating a high inference inefficiency.

We observe the inefficiency comes from two limitations of the packing algorithms in existing HE-based 2PC frameworks. On one hand, prior-art methods cannot leverage the computation characteristics of depthwise convolutions. They have to

pad the depthwise filter with zeros and convert it back to a dense filter during packing [10], [15], leading to low packing density and high computation and communication overhead. On the other hand, they often ignore the communication to transfer input and output ciphertexts are imbalanced and only focus on optimizing the input communication [10], [14], [15].

In this paper, we propose Falcon, an effective dense packing algorithm for HE-based 2PC frameworks for privacy-preserving efficient network inference. Falcon features two main techniques to reduce inference latency for depthwise and group convolutions. First, while zero padding is necessary for computation correctness, Falcon reuses the zero channels between padded filters to improve the overall packing density. Secondly, we find the output ciphertext transfer often dominates the overall communication and propose to tile the input tensor and the depthwise convolution. Although the tiling increases the input ciphertext transfer communication slightly, it drastically improves the output transfer efficiency. Our main contributions can be summarized as follows:

- We observe the bottleneck of existing HE-based 2PC frameworks when processing depthwise convolutions and propose Falcon to improve the inference efficiency of SOTA lightweight networks.
- We propose a zero-aware greedy packing algorithm, which formulates the depthwise filter packing as a shortest common superstring problem and proposes a greedy algorithm to improve the packing density.
- We propose a communication-aware operator tiling algorithm and achieve further communication reduction by balancing the input and output ciphertext transfer communication.
- Falcon outperforms SOTA HE-based 2PC frameworks, including Cheetah and Iron, with $1.4 \sim 5.4\times$ and $3.6 \sim 15.7\times$ communication reduction, respectively, at operator level, especially for high polynomial orders. With iso-latency, Falcon allows for 1.4% and 4.2% accuracy improvement on the CIFAR-100 and Tiny Imagenet datasets over Cheetah, respectively.

II. PRELIMINARIES

A. Threat Model

We focus on efficient privacy-preserving DNN inference involving two parties, i.e., server and client, in which the server holds the proprietary DNN model and the client owns private data [10], [16]. The model architecture, including the number of layers as well as the types, dimensions, and bit widths for each layer, is public to both the server and the client [9], [14], [15]. At the end of the protocol execution, the client learns the inference results without leaking any information to the server. Consistent with previous works [20]–[23], we adopt an *honest-but-curious* security model in which both parties follow the specification of the protocol but also try to learn more from the protocol than allowed.

TABLE I
NOTATIONS USED IN THE PAPER.

Notations	Meanings
$[n]$	$\{0, \dots, n - 1\}$ for a non-negative integer n
$\lceil \cdot \rceil, \lfloor \cdot \rfloor, \cdot \cdot \cdot$	Ceiling, flooring, and rounding operations
N, q	Polynomials degree, ciphertext bitwidth
\hat{a}	A polynomial and $\hat{a}[i]$ denotes the i -th coefficient of the polynomial
λ	Security parameter that measures the attack hardness
$\boxplus, \boxminus, \boxtimes$	Homomorphic addition, subtraction and multiplication
$\text{Enc}(\cdot), \text{Dec}(\cdot)$	Homomorphic encryption and decryption
H, W, C	Height, width, and channels of convolution input tensor
H', W', K	Height, width, and channels of convolution output tensor
R, G, s	Convolution kernel size, group size, and stride

B. Notations

Table I summarizes the notations used in this paper. The input, weight, and output tensors of a convolution operation are denoted as $\mathbf{X} \in \mathbb{Z}^{C \times H \times W}$, $\mathbf{W} \in \mathbb{Z}^{K \times C \times R \times R}$, and $\mathbf{Y} \in \mathbb{Z}^{K \times H' \times W'}$, where \mathbb{Z} denotes the integer domain. A convolution operation can be converted to a matrix-matrix multiplication $\mathbf{X}'\mathbf{W}'$ through the `im2col` operation [24], where $\mathbf{X}' \in \mathbb{Z}^{H'W' \times CR^2}$, $\mathbf{W}' \in \mathbb{Z}^{CR^2 \times K}$. For a group convolution, $\mathbf{W} \in \mathbb{Z}^{K \times G \times R \times R}$. When $G = 1$ and $K = C$, it becomes a depthwise convolution. We also use \mathbf{X}_i to represent the i -th channel of \mathbf{X} , i.e., $\mathbf{X}[i, :, :]$, $\mathbf{W}_{i,j}$ to represent the j -th channel of i -th filter, i.e., $\mathbf{W}[i, j, :, :]$. For simplicity, we also use \mathbf{W}_i denote $\mathbf{W}_{i,i}$.

C. HE-based 2PC Inference

We review the basic flow of HE-based 2PC inference [14], [25], [26]. The 2PC framework mainly involves two types of cryptographic primitives, including arithmetic secret sharing (ASS) and HE. For ASS, an l -bit feature x is shared by the server and the client additively as the sum of two values, say $\langle x \rangle_{2^l}^S$ and $\langle x \rangle_{2^l}^C$, and $x \equiv \langle x \rangle_{2^l}^S + \langle x \rangle_{2^l}^C$ [22]. For simplicity, we omit l in the rest of the paper. To compute the convolutions between the filter and the shared features, HE is leveraged. HE enables to compute homomorphically on the ciphertext without the need of decryption and thus, protects the data privacy. As in Table I, HE supports homomorphic addition, subtraction, and multiplication.

In Figure 2, the parameter of the i -th layer is represented as w_i , and the layer input and convolution output are denoted as x_i and y_i , respectively. During inference, the client and server hold additive shares denoted as $\langle \cdot \rangle^C, \langle \cdot \rangle^S$. The client encrypts its share as $\text{Enc}(\langle x_i \rangle^C)$ and sends it to the server. The server performs homomorphic operations to obtain the output $\text{Enc}(y_i) = (\text{Enc}(\langle x_i \rangle^C) \boxplus \langle x_i \rangle^S) \boxtimes w_i$. Blinding of y_i is done by subtracting a randomly sampled s_i from $\text{Enc}(y_i)$, and then, the result is sent to the client. The client decrypts it to obtain $\langle y_i \rangle^C = y_i - s_i$. The server outputs s_i as $\langle y_i \rangle^S$. We omit the details of the ReLU protocols and refer interested readers to [10], [15], [23]. Communication costs for a MobileNetV2 network performing secure inference on the CIFAR-100 dataset using Cheetah framework are highlighted as shown in Figure 2: linear layers contribute 498MB of communication in total,

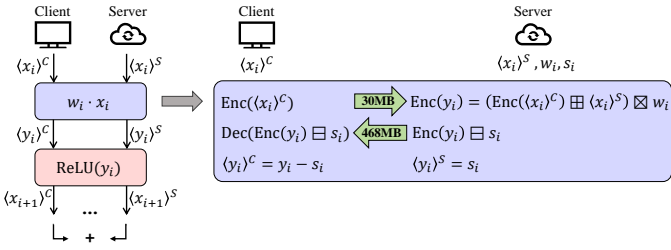


Fig. 2. Secure neural network inference based on HE (linear).

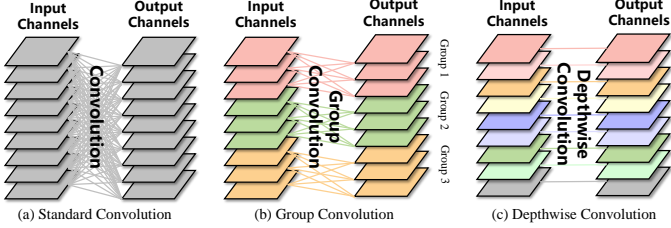


Fig. 3. (a) Standard convolution, (b) group convolution and (c) depthwise convolution.

with 30MB for input ciphertext transfer and 468MB for output ciphertext transfer.

D. Depthwise Convolution and Efficient Network

As illustrated in Figure 3, group convolution is a type of sparsely connected convolution, which is first introduced in AlexNet [27]. Standard convolution (Figure 3(a)) generates K output features by applying each filter over all C input channels, resulting in a computational cost of $O(KC)$. In contrast, group convolution (Figure 3(b)) reduces this computational cost by dividing the input channels into C/G mutually exclusive groups. Each group has G channels and produces its own set of outputs, resulting in $O(KG)$ computational cost. When $G = 1$, a group convolution becomes a depthwise convolution (Figure 3(c)), where a single filter is applied to each input channel. Depthwise convolution is widely employed in efficient networks, including MobileNetV1 [18], MobileNetV2 [1], EfficientNet-Lite [2], etc. These networks achieve SOTA accuracy with a high parameter and compute efficiency. For instance, EfficientNet-Lite achieves similar accuracy compared to ResNet50 with 4 \times latency reduction [2].

E. HE-based Convolution Protocols

Since our approach primarily focuses on the HE-based convolution layer, we first introduce how baseline methods, including CrypTFlow2 [15], Cheetah [10], and Iron [16] perform a convolution with a single input channel and single output channel (SISO).

CrypTFlow2 leverages the SIMD packing to perform HE-based convolution, which is also used by Gazelle [13], Delphi [14], etc. Figure 4 illustrates an example of using SIMD packing to accomplish SISO convolution. It requires im2col to transform a convolution into a matrix multiplication first, where $\mathbf{X}' \in \mathbb{Z}^{H'W' \times R^2}$ and $\mathbf{W}' \in \mathbb{Z}^{R^2 \times 1}$. Then each row of \mathbf{X}' is encoded into a separate ciphertext vector, denoted

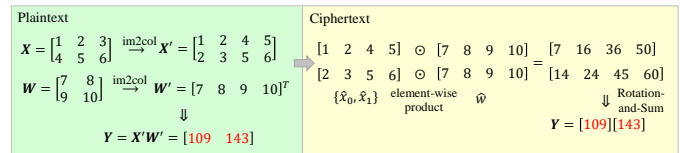


Fig. 4. Illustration of SIMD packing: rotation is required to enable summation and leads to a high computation complexity.

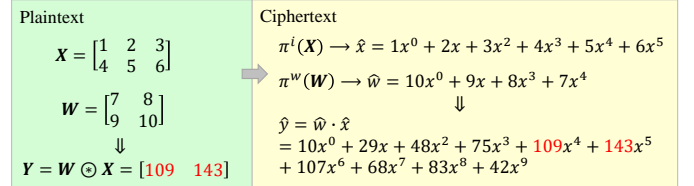


Fig. 5. Polynomial coefficient packing proposed by Cheetah.

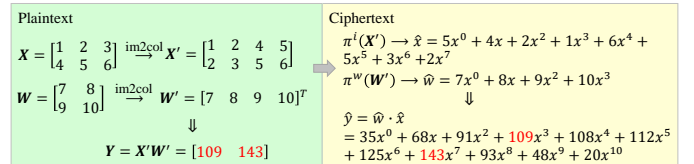


Fig. 6. Polynomial coefficient packing proposed by Iron.

as $\{\hat{x}_0, \dots, \hat{x}_{H'W'-1}\}$. \mathbf{W}' is encoded as a plaintext vector \hat{w} . With SIMD packing, a single homomorphic multiplication can realize the element-wise product between the \hat{x}_i and \hat{w} , resulting in $\hat{u}_i = \hat{x}_i \odot \hat{w}$. To further sum all the elements in \hat{u}_i , because \hat{u}_i is encrypted, it can only be re-arranged by a rotation. Hence, a “rotation-and-sum” step is needed before the final results are calculated as in Figure 4. Compared to a homomorphic multiplication, the computation complexity of a rotation is usually much higher, leading to a high computation latency [10], [13].

To get rid of the expensive rotation, Cheetah [10] discovers that a polynomial multiplication already encompasses convolution operations and proposes a polynomial coefficient encoding method [28]. Specifically, Cheetah carefully designed two mappings: π^i and π^w to convert the input and weight tensor to the polynomial coefficients, i.e., one-dimensional vectors. The two polynomials are then multiplied, and the correct convolution results can be directly extracted from the polynomial coefficients as shown in Figure 5. Iron [16] shares the same coefficient packing algorithm as Cheetah and further optimizes the algorithm for matrix-matrix multiplications. To support convolutions, Iron also requires running im2col first as shown in Figure 6.

III. INEFFICIENCY OF EXISTING SOLUTIONS FOR EFFICIENT NETWORKS

From Figure 1, we observe for prior-art 2PC frameworks, Cheetah and Iron, the computation latency of a depthwise convolution is almost the same as that of a standard convolution, indicating a high inference overhead. We now analyze the

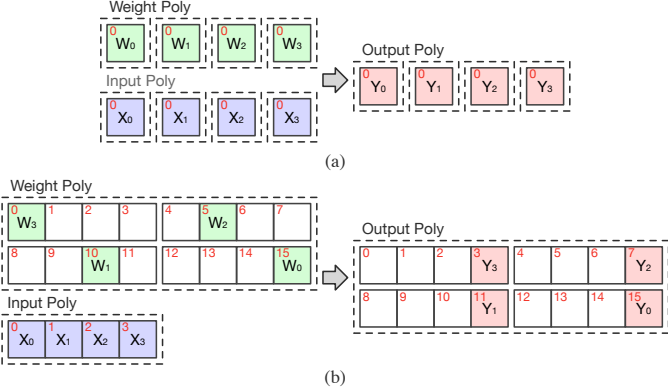


Fig. 7. Packing algorithm of (a) Iron and (b) Cheetah to support depthwise convolutions with multiple channels. Each square box represents a channel. Blank squares represent zero channels. Channels packed in the same polynomial are enclosed in the same dashed box.

origin of the overhead to shed light on the directions of further optimization. Note that we do not discuss the SIMD packing algorithm used in CrypTFlow2 as its rotation operations may result in a latency gap of over $10\times$ compared to Cheetah and Iron following [10], [16] and as shown in the experimental results. Thus, it is not the focus of our analysis.

A. Cost Analysis of HE-based Depthwise Convolution

The cost of a HE-based depthwise convolution primarily comes from computation and communication between the client and the server. The computational complexity is mainly determined by *the number of homomorphic multiplications*, while the communication consists of two parts. As in Figure 2, the first part is the transfer of input ciphertext polynomials from the client to the server, which equals to the product of the number of polynomials and the communication of each polynomial. The communication of a single polynomial scales with the polynomial degree and the bit width of each coefficient, i.e., $\#Poly \times Nq$. The second part is the transfer of output ciphertext polynomials from the server to the client. Following the optimization of Cheetah, the output transfer communication is $\#Poly \times (N+n)q$, where n is the number of output elements in each polynomial.

B. Inefficiency of Existing Packing Algorithms

In Section II-E, we have already introduced how Iron and Cheetah perform a single channel convolution and now, we focus on analyzing their complexity for multi-channel cases. For ease of explanation, we consider each channel as a basic unit and assume $HW \leq N$, i.e., each channel convolution can be packed within a polynomial. When $HW > N$, we can follow [10] to tile the input tensors.

Iron When extending to depthwise convolution with multiple channels, Iron needs to perform `im2col` operation for each channel, transforming a single depthwise convolution into C matrix multiplications. Hence, Iron generates C input polynomials, C output polynomials, and in total C homomorphic multiplications. Following Section III-A, the input transfer

communication becomes $C \times Nq$, while the output transfer communication is $C \times (N + H'W')q$. Iron only compute one channel at one time, and each input polynomial and weight polynomial only packs HW and R^2 elements, respectively, which demonstrates a high packing redundancy.

Cheetah Cheetah implements the protocol for standard convolution, and there are two approaches to extend Cheetah to support depthwise convolution. The first approach is to execute the convolution separately for each channel, which is essentially the same as Iron. A more efficient approach is to restore the depthwise convolution to a standard convolution by padding zero channels as shown in Figure 7. Then we can invoke Cheetah’s standard convolution protocol, where the non-zero channels are convolved with the input, while the zero channels can be skipped directly. The advantage of this approach is that it allows multiple channels to be packed into the same polynomial. Hence, for a depthwise convolution, Cheetah produces $\lceil \frac{CHW}{N} \rceil$ input polynomials and generates $C/\lceil \frac{N}{CHW} \rceil$ output polynomials, and requires $C/\lceil \frac{N}{CHW} \rceil$ homomorphic multiplications. The communication for input polynomials and output polynomials is $\lceil \frac{CHW}{N} \rceil Nq$ and $((C/\lceil \frac{N}{CHW} \rceil)N + CH'W')q$, respectively. Because $HW \leq N$ and $\lceil \frac{N}{CHW} \rceil \geq 1$, Cheetah’s approach is strictly superior to Iron’s approach in terms of both computation and communication. However, in Cheetah’s packing method, due to the significant amount of zero channels introduced, $\frac{C-1}{C}$ of the channels in weight polynomials are zero channels, leading to waste of compute and communication for output polynomials.

C. Inefficiency of Tiling

From the communication analysis in Section III-B, we observe that both Iron and Cheetah have a higher theoretical communication cost for output polynomials compared to input polynomials. Our experiments also confirm this observation as in Figure 2. However, both Iron and Cheetah’s tiling strategies focus on optimizing the communication cost of input polynomials: they try to pack as many input channels as possible, resulting in more compact input ciphertext. However, with the increase of the number of channels in the input polynomials, Cheetah needs to add more zero channels, which reduces the number of channels that can be packed into a weight polynomial. This further increases the number of output polynomials, and raises the output transfer communication.

IV. DEPTHWISE CONVOLUTION FRIENDLY PROTOCOL

A. Overview

We first provide an overview of our proposed method, Falcon. We build Falcon on top of Cheetah and address the significant overhead induced by the padded zero channels by two steps, including zero-aware greedy packing and communication-aware operator tiling.

B. Zero-aware Greedy Packing

As mentioned in Section III-B, the inefficiency of Cheetah arises from a significant number of packed zero channels. As shown in Figure 8, for the depthwise convolution with

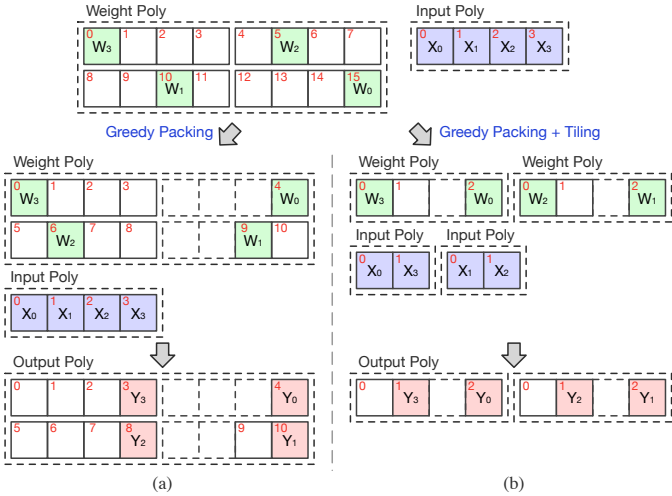


Fig. 8. Illustration of (a) zero-aware greedy packing and (b) combining zero-aware greedy packing and communication-aware operator tiling. Dashed boxes represent the zero channels reused by neighboring depthwise filters.

4 channels, after padding it to a standard convolution, the naive packing algorithm in Cheetah maps the 4 filters into $\mathbf{W}_3\mathbf{0}000\mathbf{W}_2\mathbf{0}000\mathbf{W}_1\mathbf{0}000\mathbf{W}_0$. While the padded zero channels is necessary to eliminate the interference among channels to ensure the correctness of the computation, we make the following two observations:

- The computation order of different channels does not impact the computation correctness. For example, the 4 padded filters can be mapped as $\mathbf{W}_3\mathbf{0}000\mathbf{W}_0\mathbf{0}\mathbf{W}_2\mathbf{0}000\mathbf{W}_1\mathbf{0}$ without impacting the computation of each filter.
- The zero channels of neighboring packed filters can be reused, e.g., $\mathbf{W}_3\mathbf{0}00$ can share the 3 zero channels with $000\mathbf{W}_0$, resulting in $\mathbf{W}_3\mathbf{0}00\mathbf{W}_0\mathbf{0}\mathbf{W}_2\mathbf{0}00\mathbf{W}_1\mathbf{0}$.

The above two observations enable much denser packing to drastically reduce the number of padded zero channels.

More formally, let $\mathbf{0}^{(k)}$ denote a sequence of k consecutive zero channels, then, the one-dimensional vector of i -th padded filter, denoted as $\tilde{\mathbf{W}}_i$, can be represented as $\mathbf{0}^{(C-1-i)}\mathbf{W}_i\mathbf{0}^{(i)}$, $\forall i \in [C-1]$. Let $\tilde{\mathbf{W}}$ denote the final mapping of the whole kernel, then, we observe as long as $\tilde{\mathbf{W}}_i$ is a subsequence of $\tilde{\mathbf{W}}$, the computation correctness can be guaranteed. We omit the proof due to space constraints. Let $\text{Len}(\tilde{\mathbf{W}})$ denote the vector length of the final mapping, then, we can formulate our zero-aware greedy packing as follows.

Problem 4.1: Given a set of vectors of padded filter $\{\tilde{\mathbf{W}}_0, \dots, \tilde{\mathbf{W}}_{C-1}\}$, find the optimal vector $\tilde{\mathbf{W}}$ that has the smallest length while preserving the computation correctness, i.e.,

$$\begin{aligned} & \text{minimize} \quad \text{Len}(\tilde{\mathbf{W}}) \\ & \text{s.t.} \quad \tilde{\mathbf{W}}_i \text{ is a subsequence of } \tilde{\mathbf{W}}, \forall i \in [C-1] \end{aligned}$$

Problem 4.1 is equivalent to the shortest common superstring (SCS) problem, which is proved to be NP-hard. Lots of approximation algorithms have been developed to solve the

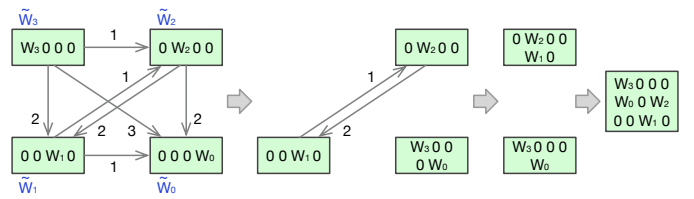


Fig. 9. Illustration of greedy algorithm for SCS problem.

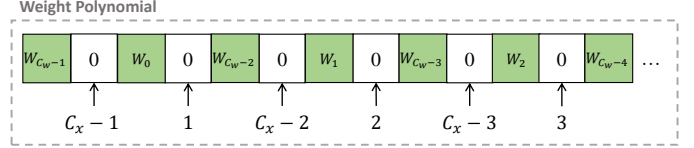


Fig. 10. Illustration of how zero-aware greedy packing combines multiple channels.

problem. We use Ukkonen's 1990 algorithm [29]. As shown in Figure 9. First, we build a directed graph where vertices are $\{\tilde{\mathbf{W}}_0, \tilde{\mathbf{W}}_1, \dots, \tilde{\mathbf{W}}_{C-1}\}$, and the weight of the edge from $\tilde{\mathbf{W}}_i$ to $\tilde{\mathbf{W}}_j$ is the length of the longest suffix zero channels of $\tilde{\mathbf{W}}_i$, which is also a prefix zero channels of $\tilde{\mathbf{W}}_j$. Next, we randomly select one of the longest edges and merge the nodes at both ends of the edge to form a new node and update the graph. Repeat this selecting and merging process until there are no more edges in the graph. Finally, merge the remaining nodes together to obtain the results $\tilde{\mathbf{W}}$.

After applying the greedy algorithm, we discover that the solution always merges the $\tilde{\mathbf{W}}_i$ and $\tilde{\mathbf{W}}_{C-1-i}$ since they are symmetric in the location of zero channels. Furthermore, if the sequence starts with zeros, those zeros can be removed without affecting the corresponding coefficients in the output. Based on the observation, we now formally derive the mapping function for our greedy packing algorithm described above. Suppose an input polynomial packs C_x channels, and a weight polynomial packs C_w channels. The sequence of weight polynomials is illustrated in Figure 10. Under the same N , we have $C_x \geq C_w$ because additional zero channels need to be added for the weight polynomials. Therefore, we let $C_x = kC_w$, where $k \in \mathbb{Z}^+$, to prevent the channels corresponding to a weight polynomial from being distributed across different input polynomials, which would result in a doubling of the homomorphic multiplications. Now, we present the coefficient mappings π_{dwconv}^i and π_{dwconv}^w to pack the three-dimensional input and weight tensors into one-dimensional vector. For simplicity, we require $\max(C_x \times H \times W, C_w \times R \times R) \leq N$, $C_x = C_w$ and C_w is even.

$$\begin{aligned} \hat{x} &= \pi_{\text{dwconv}}^i(\mathbf{X}) \text{ st. } \hat{x}[cHW + iW + j] = \mathbf{X}[c, i, j] \\ \hat{w} &= \pi_{\text{dwconv}}^w(\mathbf{W}) \text{ st. } \hat{w}[\text{offset}(c') \times HW + O - lW - l'] \\ &= \mathbf{W}[c', l, l'] \end{aligned}$$

where $O = W(h-1) + h - 1$ and offset is:

$$\text{offset}(c') = \begin{cases} (C_x + 2) \times (C_w - 1 - c'), & c' \geq \frac{C_w}{2} \\ C_x + c' \times (C_x + 1), & c' < \frac{C_w}{2} \end{cases}$$

The multiplication $\hat{y} = \hat{x} \cdot \hat{w}$ directly gives the 2-dimension depthwise convolution in some of the coefficients of the resulting polynomial:

$$\mathbf{Y}[k', i', j'] = \hat{y} [(\text{offset}(k') + k') \times HW + O + i'sW + j's]$$

where $\mathbf{Y} \in \mathbb{Z}^{C_x \times H' \times W'}$. $\text{offset}(k')$ calculates the offset of weights at the channel level, while k' calculates the offset of inputs at the channel level. This is used to determine the starting position of each output channel, while the encoding within a single channel remains consistent with Cheetah.

When $k \neq 1$, it means that the same input polynomial \hat{x} needs to be multiplied with multiple weight polynomials $\{\hat{w}_0, \hat{w}_1, \dots, \hat{w}_{k-1}\}$ to obtain the outputs $\{\hat{y}_0, \hat{y}_1, \dots, \hat{y}_{k-1}\}$. In order to perform packing in this case, we first concatenate these weight polynomials end-to-end to form a larger polynomial $\hat{w} = \hat{w}_0\hat{w}_1\dots\hat{w}_{k-1}$. Then, we apply packing to \hat{w} , and \hat{w} still satisfies $\hat{w} = \pi_{\text{dwconv}}^w(\mathbf{W})$. Afterwards, \hat{w} is divided into k smaller polynomials, and the leading zeros of each polynomial are removed.

Complexity Analysis. Now we analyze the computational and communication complexity of zero-aware greedy packing theoretically. We first analyze the utilization of weight polynomial coefficients. Evidently, Cheetah’s utilization rate is $\frac{1}{C_x}$. Based on the analysis shown in Figure 10, our theoretical utilization is $\frac{C_w}{C_x+1+(C_w/2-1)(C_x+2)} > \frac{2}{C_x+2}$. Considering the range of values for C_x in neural networks, zero-aware greedy packing can achieve approximately twice the channel utilization rate compared to Cheetah.

In terms of computational complexity, zero-aware greedy packing reduces the number of polynomial multiplications by a factor of $\frac{2}{C_x+2}$ compared to Cheetah. As for communication, zero-aware greedy packing reduces the communication of the output polynomials from $(\lceil \frac{C_xHW}{N} \rceil N + C_xH'W')q$ to $(\lceil \frac{(C_x+2)HW}{2N} \rceil N + C_xH'W')q$ compared with Cheetah. In Section III-B, it has been proven that the computational and communication complexity of Cheetah is strictly superior to Iron. Therefore, our method outperforms both Cheetah and Iron in computation and communication.

C. Communication-aware Operator Tiling

As shown in Figure 2, the communication of the output polynomials is much higher than that of the input polynomials. This observation aligns with the communication cost formula derived in Section III-B. Previous algorithms aim to maximize the number of channels packed in one input polynomial (C_x) [10], [13]–[16], but this leads to reduced utilization of weight polynomial coefficients and smaller C_w because more zero channels need to be padded. Moreover, the reduction in C_w significantly increases the communication cost of output polynomials, resulting in excessively high communication costs.

To address this issue, we propose a novel communication-aware operator tiling method. Unlike previous methods, we conduct a theoretical analysis of communication cost in depthwise convolution and formulate it as a nonlinear programming problem. Our objective is to minimize communication while

adhering to polynomial coefficient encoding rules. Formally, the communication cost is given by the equation:

$$\lceil \frac{C}{C_x} \rceil Nq + \lceil \frac{C}{C_w} \rceil (N + H'W'C_w)q$$

The first part of the equation represents the communication of the input polynomials, where $\lceil \frac{C}{C_x} \rceil$ is the number of ciphertexts. The second part corresponds to the output polynomials communication as discussed in Section III-B. By approximating the ceiling function as $\lceil x \rceil \approx x$, we obtain:

$$NCq\left(\frac{1}{C_x} + \frac{1}{C_w}\right) + H'W'Cq$$

Among them, only $\frac{1}{C_x} + \frac{1}{C_w}$ needs to be minimized, with all other parameters known before executing the convolution protocol. We also have two constraints: 1) polynomial coefficient encoding should not exceed the degree N , and 2) C_x must be a positive integer multiple of C_w . Hence, we can formulate the communication optimization problem as follows:

$$\begin{aligned} &\text{minimize} && \left\| \frac{1}{C_x} + \frac{1}{C_w} \right\| \\ &\text{s.t.} && (C_x + 2)C_w \leq \frac{2N}{HW} + 2 \\ &&& C_x = kC_w \text{ where } k \in \mathbb{Z}^+ \end{aligned}$$

This is a solvable nonlinear programming problem with a relatively small solution space. With $C_x \leq \frac{N}{HW}$ and $C_x = kC_w$, the solution space is at most $\frac{N}{HW} \times \frac{N}{HW}$, allowing us to directly solve it using a search algorithm with a complexity of $O((\frac{N}{HW})^2)$. An example is illustrated in Figure 8 (b), after tiling, we reduce the size of weight polynomials and output polynomials.

D. Extending to group convolution

Furthermore, we discover that our method can be naturally extended to group convolution. In group convolution, C convolutional filters are divided into $\frac{C}{G}$ groups, with each group containing G convolutional filters, and each filter consisting of G channels. In this case, instead of treating individual channels or filters as basic units, we consider a whole group of convolutional filters (including G kernels and G^2 channels) as a basic unit. The packing between groups follows the rules of zero-aware greedy packing, while within each group, it essentially becomes a standard convolution and can be directly packed using the Cheetah approach for standard convolutions.

V. EXPERIMENTAL RESULTS

A. Experimental Setup

Falcon is built on top of the SEAL library [30], the EMP toolkit [31] and OpenCheetah [10] in C++. We also use the Ezpc library [32] to evaluate CrypTFlow2 [15]. Consistent with [22], [33], we simulate a WAN network setting via Linux Traffic Control, where the bandwidth is 9 MBps. All the following experiments are performed on machines with 2.2 GHz Intel Xeon CPU and 256GB RAM. Following [10], [16], we set $N = 4096$ for most of the cases.

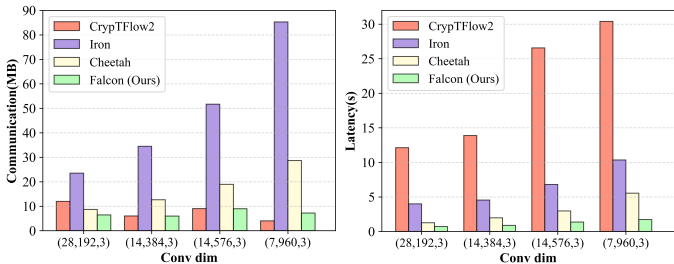


Fig. 11. (a) Communication and (b) latency comparison of depthwise convolutions of different dimensions (the tuple represents the input feature height, channels, and kernel size).

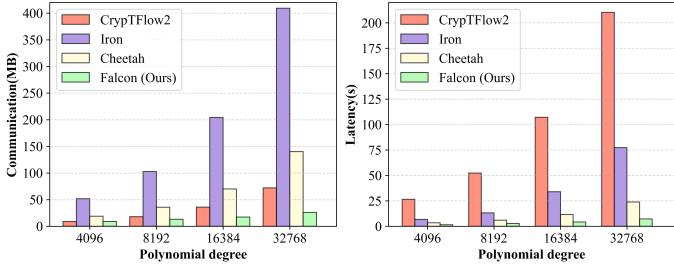


Fig. 12. (a) Communication and (b) latency comparison of a depthwise convolution under different polynomial degrees.

B. Microbenchmark Evaluation

a) Single Depthwise Convolution Evaluation: We compare the performance of Falcon with CrypTFlow2, Iron, and Cheetah for a single depthwise convolution. As shown in Figure 11, Falcon achieves a communication reduction of $1.4 \sim 4.0 \times$ and a latency reduction of $1.8 \sim 3.2 \times$ compared to Cheetah. Compared to Iron, Falcon achieves a communication reduction of $3.6 \sim 11.8 \times$. It is important to note that CrypTFlow2 (with SIMD) has relatively low communication. However, as mentioned in Section III, the SIMD method has high computational complexity, resulting in significant latency. In comparison, our method achieves a latency reduction of $15.6 \sim 19.9 \times$.

b) Depthwise Convolution under Different Polynomial Degree: We benchmark Falcon against CrypTFlow2, Cheetah, and Iron, for different polynomial degrees. We select a depthwise convolution with input dimension of $(14, 576, 3)$ for evaluation. As shown in Figure 12, overall, with the increase of N , Falcon achieves a higher speedup compared to existing methods due to a larger packing optimization space. Compared to Cheetah, we achieve a communication reduction of $4.0 \times$ at $N = 4096$ and an even greater reduction of $11.1 \times$ at $N = 32768$. Compared to Iron, our method achieves a remarkable communication reduction of $32.9 \times$ when $N = 32768$.

c) Depthwise Convolution under Different Bandwidth:

We also benchmark the latency of Falcon against CrypTFlow2, Cheetah, and Iron under different bandwidth settings: 9Mbps, 44Mbps, and 384Mbps, representing WAN settings in [22], [33], WAN and LAN settings in Cheetah [10], respectively. In Table II, our methods achieve a significant latency reduction

TABLE II
LATENCY (S) COMPARISON UNDER DIFFERENT BANDWIDTHS.

Bandwidth	Methods			
	CrypTFlow2	Iron	Cheetah	Falcon (ours)
384MB/s [10]	29.66	10.23	2.44	0.43
44MB/s [10]	30.24	10.49	3.04	0.45
9MB/s [22], [33]	30.86	10.68	5.56	0.76

TABLE III
COMMUNICATION (MB) COMPARISON UNDER DIFFERENT GROUP SIZES.

Group size	Methods			
	CrypTFlow2	Iron	Cheetah	Falcon (ours)
1	9.00	51.70	18.94	8.98
2	9.00	51.70	18.94	8.98
4	9.00	68.44	18.94	8.98
8	9.00	102.73	18.94	8.98

of approximately $5.6 \sim 7.35 \times$ compared to Cheetah, and this advantage increases as the bandwidth decreases. We also observe that CrypTFlow2 and Iron are not sensitive to bandwidth. For CrypTFlow2, this is because it suffers from a high computational complexity while for Iron, we hypothesize the latency bottleneck comes from the frequent encryption and decryption.

d) Group Convolution Evaluation: We also evaluate the performance of Falcon for group convolutions. We select a depthwise convolution with dimension of $(14, 576, 3)$ and benchmark its performance under different group sizes. As shown in Table III, our method consistently achieves better communication for different group sizes. Additionally, we notice that, except for Iron, the other methods are not sensitive to the group size. The main reason is that both CrypTFlow2 and Cheetah expand group convolutions into standard convolutions. In contrast, Iron's approach leads to an increase in matrix multiplication dimension as the group size grows. When the dimension exceed the polynomial degree N , it results in a significant increase of communication.

C. End-to-end Inference Evaluation

a) Communication and Latency Comparison: We now perform an end-to-end inference evaluation compared to prior-art methods, including CrypTFlow2 and Cheetah. Due to the unavailability of open-source code for Iron, we find it difficult to reproduce all of its linear and nonlinear protocols. As a result, we are unable to evaluate its performance in the end-to-end inference. We apply Falcon to two widely used efficient networks, MobileNetV2 and EfficientNet-lite, and evaluate their performance on the Cifar10, Cifar100 [34], and Tiny Imagenet [35] datasets. We set the bandwidth to 9Mbps and $N = 4096$.

Results and analysis. As shown in Table IV, compared to Cheetah, Falcon reduces the communication by $1.31 \times$ and the latency by more than $1.2 \times$ on the Cifar10 and Cifar100 datasets. On the Tiny Imagenet dataset, the advantage of Falcon is greater, with a communication reduction of

TABLE IV

END-TO-END COMPARISON WITH PRIOR-ART WORKS ON DIFFERENT ARCHITECTURES AND DATASETS (THE INFERENCE COMPLEXITY ON CIFAR10 AND CIFAR100 IS ESSENTIALLY THE SAME).

Network	Dataset	CrypTFlow2		Cheetah		Falcon (Ours)	
		Comm. (GB)	Latency (s)	Comm. (GB)	Latency (s)	Comm. (GB)	Latency (s)
MobileNetV2	Cifar	2.32	622.43	0.60	132.03	0.46	109.27
MobileNetV2	Tiny Imagenet	2.42	1067.34	0.70	168.35	0.54	130.41
EfficientNet-lite	Cifar	0.83	563.90	0.50	103.48	0.34	76.61
EfficientNet-lite	Tiny Imagenet	1.28	915.36	0.64	146.37	0.45	107.44

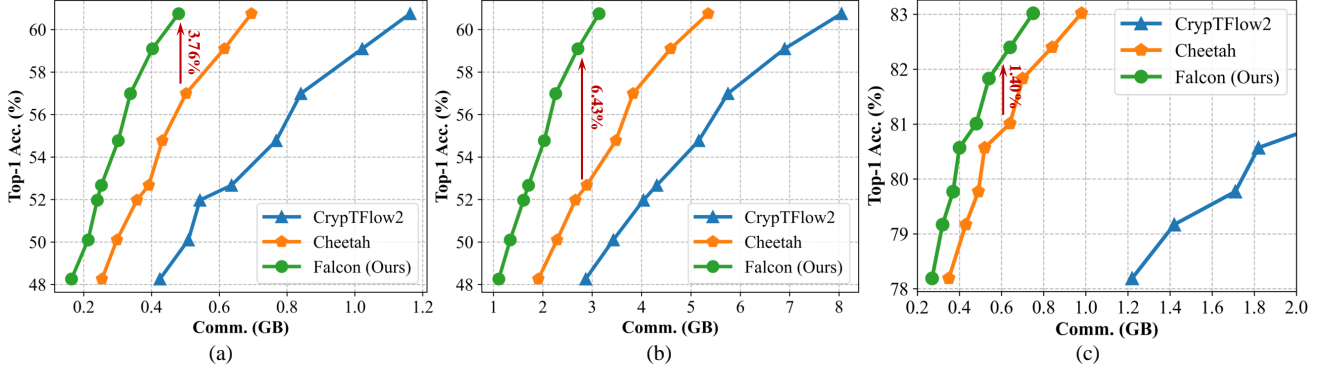


Fig. 13. Accuracy comparison with Cheetah and CrypTFlow2 on (a) Tiny Imagenet, $N=4096$; (b) Tiny Imagenet, $N=32768$; (c) Cifar-100, $N=4096$.

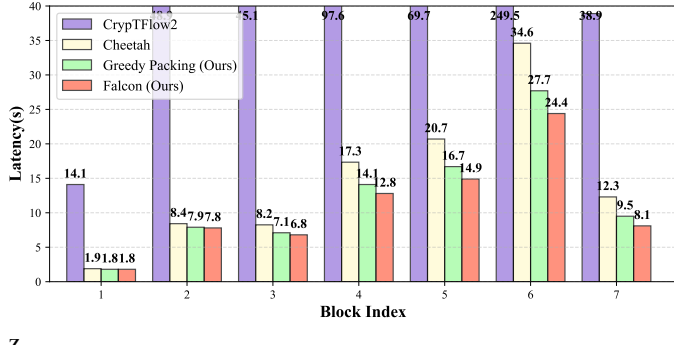


Fig. 14. Block-wise comparison of latency on MobileNetV2/TinyImagenet, $N=4096$.

1.44 \sim 1.48 \times and a latency reduction of 1.35 \sim 1.36 \times . These experimental results resonate with the theoretical expectations. For Tiny Imagenet, the networks have more layers which have smaller dimensions H and W but larger channel size C , resulting in a larger packing optimization space.

b) *Networks Accuracy Comparison*: We also benchmark the accuracy of MobileNetV2 networks with different channel-widths on Cifar100 and Tiny Imagenet for CrypTFlow2, Cheetah, and Falcon (Ours). Additionally, we select $N = 4096$ and $N = 32768$ to demonstrate the superiority of our method with larger N .

Results and analysis. As shown in Figure 13, Falcon consistently outperforms the other methods across different network widths. In Tiny Imagenet, when $N = 4096$, with approximately 0.5GB of communication costs, Falcon achieves 60.75% top-1 accuracy, surpassing Cheetah and CrypTFlow2

by 3.76% and 10.65%, respectively. When N is further increased to 32768, Falcon maintains a substantial lead in top-1 accuracy over Cheetah and CrypTFlow2. With approximately 2.8GB of communication, Falcon outperforms them by 6.43% and 10.81%, respectively. For the Cifar100 dataset, as the network exhibits strong capability on it, increasing the width does not bring significant accuracy improvement. However, Falcon still achieves an average accuracy improvement of 1.4%.

c) *Block-wise Latency Comparison*: We show the block-wise latency comparison in Figure 14. As we can observe, Falcon achieves more latency reduction in deeper layers of the network, as H, W becomes smaller and C becomes larger, resulting in a larger packing optimization space. Additionally, Falcon reduces the latency for all the blocks, highlighting the effectiveness of Falcon.

VI. CONCLUSION

In this paper, we propose Falcon, a dense packing algorithm for homomorphically encrypted depthwise and group convolution for HE-based 2PC network inference. Falcon leverages the computation characteristics of the depthwise convolution and directly optimize the communication bottleneck. Falcon features a zero-aware greedy packing algorithm and a communication-aware operator tiling strategy to significantly reduce the communication for efficient networks. Compared with prior-art works, e.g., Cheetah and Iron, Falcon achieves a latency reduction of 1.8 \sim 3.2 \times at the operator level and 1.21 \sim 1.36 \times at the network level, which translates to 1.4% and 4.2% accuracy improvement with iso-communication. These improvements enhance the practicality of HE-based 2PC inference for efficient networks.

REFERENCES

- [1] M. Sandler, A. Howard, M. Zhu, A. Zhmoginov, and L.-C. Chen, “Mobilenetv2: Inverted residuals and linear bottlenecks,” in *IEEE/CVF conference on computer vision and pattern recognition (CVPR)*, 2018, pp. 4510–4520.
- [2] M. Tan and Q. Le, “Efficientnet: Rethinking model scaling for convolutional neural networks,” in *International conference on machine learning (ICML)*. PMLR, 2019, pp. 6105–6114.
- [3] Z. Liu, H. Mao, C.-Y. Wu, C. Feichtenhofer, T. Darrell, and S. Xie, “A convnet for the 2020s,” in *IEEE/CVF Conference on Computer Vision and Pattern Recognition (CVPR)*, 2022, pp. 11976–11986.
- [4] N. Azouji, A. Sami, and M. Taheri, “Efficientmask-net for face authentication in the era of covid-19 pandemic,” *Signal, Image and Video Processing*, vol. 16, no. 7, pp. 1991–1999, 2022.
- [5] G. Kaassis, A. Ziller, J. Passerat-Palmbach, T. Ryffel, D. Usynin, A. Trask, I. Lima Jr, J. Mancuso, F. Jungmann, M.-M. Steinborn *et al.*, “End-to-end privacy preserving deep learning on multi-institutional medical imaging,” *Nature Machine Intelligence*, vol. 3, no. 6, pp. 473–484, 2021.
- [6] W.-S. Choi, B. Reagen, G.-Y. Wei, and D. Brooks, “Impala: Low-latency, communication-efficient private deep learning inference,” May 2022.
- [7] D. Demmler, T. Schneider, and M. Zohner, “Aby -a framework for efficient mixed-protocol secure two-party computation,” in *Proceedings 2015 Network and Distributed System Security Symposium*, Feb 2015. [Online]. Available: <http://dx.doi.org/10.14722/ndss.2015.23113>
- [8] K. Gupta, D. Kumaraswamy, N. Chandran, and D. Gupta, “Llama: A low latency math library for secure inference,” *Proceedings on Privacy Enhancing Technologies*, vol. 2022, no. 4, p. 274–294, Sep 2022. [Online]. Available: <http://dx.doi.org/10.56553/popeps-2022-0109>
- [9] N. Kumar, M. Rathee, N. Chandran, D. Gupta, A. Rastogi, and R. Sharma, “Cryptflow: Secure tensorflow inference.” in *2020 IEEE Symposium on Security and Privacy (SP)*, Jul 2020. [Online]. Available: <http://dx.doi.org/10.1109/sp40000.2020.00092>
- [10] Z. Huang, W.-j. Lu, C. Hong, and J. Ding, “Cheetah: Lean and fast secure {Two-Party} deep neural network inference,” in *31st USENIX Security Symposium (USENIX Security 22)*, 2022, pp. 809–826.
- [11] R. Rathathri, O. Saarikivi, H. Chen, K. Laine, K. Lauter, S. Maleki, M. Musuvathi, and T. Mytkowicz, “Chet: an optimizing compiler for fully-homomorphic neural-network inferencing,” in *Proceedings of the 40th ACM SIGPLAN Conference on Programming Language Design and Implementation*, Jun 2019. [Online]. Available: <http://dx.doi.org/10.1145/3314221.3314628>
- [12] D. Kim, J. Park, J. Kim, S. Kim, and J. Ahn, “Hyphen: A hybrid packing method and optimizations for homomorphic encryption-based neural networks,” Feb 2023.
- [13] C. Juvekar, V. Vaikuntanathan, and A. Chandrakasan, “GAZELLE: A low latency framework for secure neural network inference,” Jan 2018.
- [14] P. Mishra, R. Lehmkuhl, A. Srinivasan, W. Zheng, and R. Popa, “Delphi: A cryptographic inference service for neural networks,” Jan 2020.
- [15] D. Rathee, M. Rathee, N. Kumar, N. Chandran, D. Gupta, A. Rastogi, and R. Sharma, “Cryptflow2: Practical 2-party secure inference,” in *Proceedings of the 2020 ACM SIGSAC Conference on Computer and Communications Security*, 2020, pp. 325–342.
- [16] M. Hao, H. Li, H. Chen, P. Xing, G. Xu, and T. Zhang, “Iron: Private inference on transformers,” in *Advances in Neural Information Processing Systems*, 2022.
- [17] Q. Lou and L. Jiang, “Hemet: A homomorphic-encryption-friendly privacy-preserving mobile neural network architecture,” May 2021.
- [18] A. G. Howard, M. Zhu, B. Chen, D. Kalenichenko, W. Wang, T. Weyand, M. Andreetto, and H. Adam, “Mobilenets: Efficient convolutional neural networks for mobile vision applications,” *arXiv preprint arXiv:1704.04861*, 2017.
- [19] M. Tan and Q. Le, “Efficientnetv2: Smaller models and faster training,” in *International conference on machine learning*. PMLR, 2021, pp. 10096–10106.
- [20] R. Gilad-Bachrach, N. Dowlin, K. Laine, K. Lauter, M. Naehrig, and J. Wernsing, “Cryptonets: Applying neural networks to encrypted data with high throughput and accuracy,” in *International conference on machine learning*. PMLR, 2016, pp. 201–210.
- [21] S. U. Hussain, M. Javaheripi, M. Samragh, and F. Koushanfar, “Coinn: Crypto/ml codesign for oblivious inference via neural networks,” in *Proceedings of the 2021 ACM SIGSAC Conference on Computer and Communications Security*, 2021, pp. 3266–3281.
- [22] P. Mohassel and Y. Zhang, “Secureml: A system for scalable privacy-preserving machine learning,” in *2017 IEEE Symposium on Security and Privacy (SP)*, Jun 2017.
- [23] D. Rathee, M. Rathee, R. K. K. Goli, D. Gupta, R. Sharma, N. Chandran, and A. Rastogi, “Sirnn: A math library for secure rnn inference,” in *2021 IEEE Symposium on Security and Privacy (SP)*. IEEE, 2021, pp. 1003–1020.
- [24] K. Chellapilla, S. Puri, and P. Simard, “High performance convolutional neural networks for document processing,” in *Tenth international workshop on frontiers in handwriting recognition*. Suvisoft, 2006.
- [25] J. Liu, M. Juuti, Y. Lu, and N. Asokan, “Oblivious neural network predictions via minionna transformations,” in *Proceedings of the 2017 ACM SIGSAC Conference on Computer and Communications Security*, Oct 2017.
- [26] K. Garimella, Z. Ghodsi, N. Jha, S. Garg, and B. Reagen, “Characterizing and optimizing end-to-end systems for private inference,” Jul 2022.
- [27] A. Krizhevsky, I. Sutskever, and G. E. Hinton, “Imagenet classification with deep convolutional neural networks,” *Communications of the ACM*, vol. 60, no. 6, pp. 84–90, 2017.
- [28] S. Bian, D. E. S. Kundi, K. Hirozawa, W. Liu, and T. Sato, “Apas: application-specific accelerators for rlwe-based homomorphic linear transformations,” *IEEE Transactions on Information Forensics and Security*, vol. 16, pp. 4663–4678, 2021.
- [29] E. Ukkonen, “A linear-time algorithm for finding approximate shortest common superstrings,” *Algorithmica*, vol. 5, no. 1-4, pp. 313–323, 1990.
- [30] “Microsoft SEAL (release 3.6).” <https://github.com/Microsoft/SEAL>, Nov. 2020, microsoft Research, Redmond, WA.
- [31] X. Wang, A. J. Malozemoff, and J. Katz, “EMP-toolkit: Efficient MultiParty computation toolkit,” <https://github.com/emp-toolkit>, 2016.
- [32] N. Chandran, D. Gupta, A. Rastogi, R. Sharma, and S. Tripathi, “Ezpc: Programmable, efficient, and scalable secure two-party computation for machine learning,” *Cryptology ePrint Archive*, 2017.
- [33] L. Shen, Y. Dong, B. Fang, J. Shi, X. Wang, S. Pan, and R. Shi, “Abnn 2,” in *Proceedings of the 59th ACM/IEEE Design Automation Conference*, Aug 2022.
- [34] A. Krizhevsky, G. Hinton *et al.*, “Learning multiple layers of features from tiny images,” 2009.
- [35] J. Deng, W. Dong, R. Socher, L.-J. Li, K. Li, and L. Fei-Fei, “Imagenet: A large-scale hierarchical image database,” in *2009 IEEE conference on computer vision and pattern recognition*. Ieee, 2009, pp. 248–255.